CRYSTAL GROWTH & DESIGN

Article

Cite This: *Cryst. Growth Des.* 2018, 18, 6302−6306

pubs.acs.org/crystal

In Silico Crystal Growth Rate Prediction for NaCl from Aqueous Solution

Mark N. Joswiak,[†] Baron Peters,[*,†,‡] and Michael F. Doherty[*,†]

[†]Department of Chemical Engineering and [‡]Department of Chemistry and Biochemistry, University of California, Santa Barbara, United States

Supporting Information

ABSTRACT: The prediction of crystal growth rates from solution is a longstanding challenge and paramount opportunity for pharmaceuticals, materials science, biomineralization, and beyond. This work overcomes the key obstacle by calculating solute attachment rates to the crystal surface via atomistic simulations and rare-event methods. These rates are combined with the multiscale spiral growth model to produce the first parameter-free in silico crystal growth rate predictions. Our results are in excellent agreement with experimental measurements for sodium chloride grown from aqueous solution.

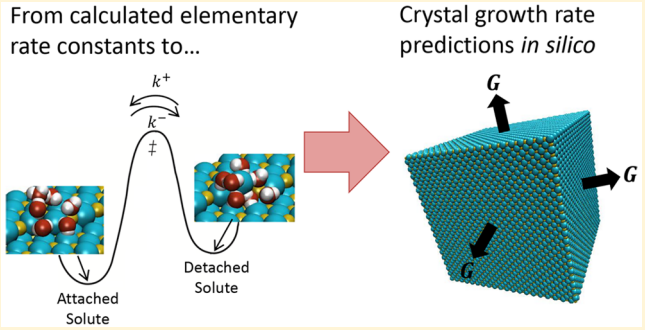

INTRODUCTION

Crystal growth rates depend on crystal features and processes that span a wide range of length and time scales. Figure 1 shows how these processes are coupled for spiral growth, the predominant mechanism at low supersaturation. Closed-form rate equations exist for all events in the hierarchy except for the attachment of solute growth units to surface kink sites (orange box in Figure 1). As shown in Figure 1, kinks are exposed half-lattice sites that regenerate upon solute attachment; that is, they are the "catalytic sites" for growth. Special molecular simulation methods are required to overcome the long time scales between kink attachment events, especially for ionic crystals, where the desolvation process can be rate-limiting.[1] Several computational studies have examined solute attachment,[2−6] but only a few have focused on kink sites,[4−6] and kink attachment rates have never been calculated. A key challenge in computing the kink attachment rate, resolved in this work, is the arbitrary boundary between the states with the solute attached to the crystal and with the solute in bulk solution.

We previously computed the rates and free energy barriers for ion *detachment* from kink sites for NaCl dissolution into pure water, and we also elucidated the mechanistic role of desolvation.[4] In principle, it should be possible to predict *growth* rates from the dissolution kinetics and the saturation limit, but the inversion is complicated by the multiscale nature of spiral growth. Here, we develop the theoretical framework to compute kink *attachment* rates, which we implement in the spiral growth model. Our results demonstrate that accurate in silico crystal growth rate predictions are now possible, even when solute attachment is an activated process and when the available force fields are imperfect.

SPIRAL CRYSTAL GROWTH

At low supersaturations, faceted crystals grow via the spiral mechanism (Figure 1), wherein a rotating spiral emanates from a screw dislocation at the surface.[7] The growth rate depends on the spiral rotation time, which creates a new crystal layer.[7,8] For a cubic NaCl crystal, all faces are identical (the {001} family), and all spirals contain four equivalent edges, that is, the [100] edge on the (001) face, with alternating Na^+ and Cl^- (see Figure 1). This symmetry results in the crystal face growth rate (e.g., in nm/s)

$$G_{\mathrm{NaCl}} = \frac{a_{\mathrm{P}}\rho u h}{4 l_{\mathrm{c}}} \tag{1}$$

where h = 0.28 nm is the height of a new layer (half the unit cell dimension), a_{P} = 0.28 nm is the propagation length upon completion of a new row along the edge, ρ is the density of kink sites along the edge, u is the kink velocity (net frequency of ion attachment to a kink site), and l_{c} is the critical spiral edge length. We first focus on the calculation of u before discussing ρ and l_{c}.

ION ATTACHMENT RATES

The attachment/detachment of an ion at a kink site is a two-event process (see Figure 2) in which ions make transitions between three states:

- **B**: ion in bulk solution.
- **D**: ion docked nearby the kink site.
- **I**: ion incorporated into the kink site.

Received: August 6, 2018
Published: August 30, 2018

DOI: 10.1021/acs.cgd.8b01184
Cryst. Growth Des. 2018, 18, 6302−6306

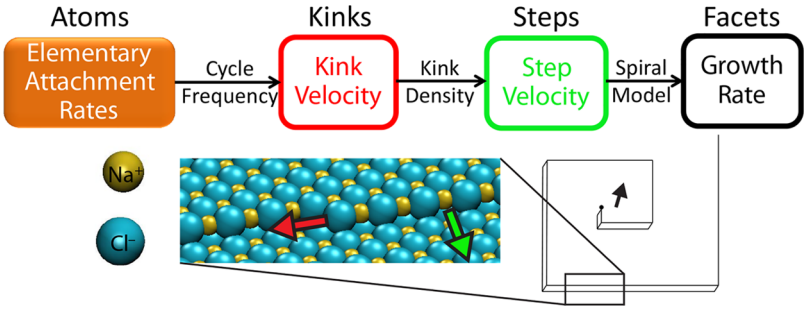

Figure 1. Schematic diagram of the multiscale crystal growth model approach, illustrating the connections between the various crystal features and rates from individual atoms/solutes to macroscopic crystal faces. A rotating spiral is shown along with a close-up image of a NaCl edge with a single kink site (Na^+ is yellow and Cl^- is teal). The arrows indicate the movement direction of the kink (red), the step front (green), and the facet (black; out of the page).

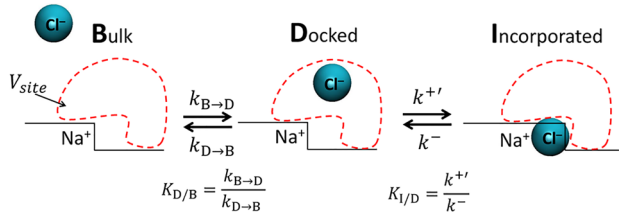

Figure 2. Schematic diagram of the attachment/detachment pathway for Cl^- at a kink site. The black line represents the step front, which progresses up the page during growth.

Along the attachment pathway, the first event is docking, wherein an ion goes from bulk solution (**B**) to a docked/adsorbed state (**D**) nearby the kink site. Then, the ion enters the kink site, that is, the incorporated state (**I**). Note that state **I** for Cl^- corresponds to state **B** for Na^+, so the overall growth process resembles a catalytic cycle with a traveling active site.

Our previous paper described the mechanism of ion detachment (including solvation) from a kink site. Free energy calculations in that work showed that Na^+ and Cl^- have little, if any, affinity for their docked states[4] (see Figure S3 in the Supporting Information). Accordingly, there is no well-defined boundary between **B** and **D**, which complicates the attachment rate calculation. To facilitate the calculation, we define an arbitrary docked state volume V_{site} (red outline in Figure 2) that ultimately vanishes from the overall rate expression—a technique borrowed from the catalysis literature.[9]

The docking event involves ion diffusion into the V_{site} region. The docking and undocking rates are, respectively, $k_{B\to D}C\theta_B$ and $k_{D\to B}\theta_D$, where the docking and undocking rate constants are $k_{B\to D}$ and $k_{D\to B}$, C is the molarity of the ion in bulk solution, and θ_i is the probability of being in state i. Each term in these rate expressions is specific to a particular ion and kink site, and thus each quantity has corresponding Na^+ and Cl^- values. Docking is much faster than incorporation (verified later), so we invoke the quasi-equilibrium assumption between states **B** and **D**. This leads to $\theta_D = CV_{site}$; that is, θ_D is the small Poisson probability of finding one ion in the small volume V_{site} (see Supporting Information).

After the ion docks, the kink site must desolvate prior to ion attachment. This incorporation event is rate-limiting, and therefore the overall kink attachment and detachment rates are (respectively)

$$j^+ = k^{+\prime}\theta_D = (k^{+\prime}V_{site})C \quad (2)$$

$$j^- = k^- \quad (3)$$

where $k^{+\prime}$ is the attachment rate constant for the incorporation event, and k^- is the detachment rate constant. As we will show, j^+ is independent of V_{site}, because $k^{+\prime}$ is proportional to $1/V_{site}$. We previously computed k^- for Na^+ and Cl^- (Table 1).[4] Here,

Table 1. Computed Kink Attachment and Detachment Rate Constants for NaCl in Water

ion	k^+ (L/mol/s)	k^- (1/s)	$\beta\Delta W$
Na^+	$2.6 \pm 0.3 \times 10^8$	$1.6 \pm 0.2 \times 10^8$	4.5 ± 0.2
Cl^-	$7.6 \pm 1.2 \times 10^5$	$6.3 \pm 0.8 \times 10^6$	1.9 ± 0.2

we compute the incorporation rate constant via $k^{+\prime} = k^-K_{I/D}$, where $K_{I/D}$ is the equilibrium constant between **I** and **D**. Our approach includes the desolvation barrier for attachment, because we previously accounted for desolvation in the detachment (k^-) rate constants for Na^+ and Cl^-.

We compute the partition functions Q in the docked and incorporated states to determine the equilibrium constant $K_{I/D} = Q_I/Q_D$. For each ion, Q_I and Q_D can be obtained from the potential of mean force (PMF) as a function of distance r between the ion and the kink site. See the Supporting Information for details on the PMF and the partition function calculations, which also verifies that j^+ is independent of V_{site}.

For consistency with convention, we define an overall rate constant k^+, such that eq 2 becomes $j^+ = k^+C$. We find that the attachment rate constant for Na^+ ($k^+_{Na} = 2.6 \times 10^8$ L/mol/s) is over 2 orders of magnitude larger than the Cl^- attachment rate constant ($k^+_{Cl} = 7.6 \times 10^5$ L/mol/s). Thus, NaCl crystal growth is limited by Cl^- attachment. We also previously showed that Cl^- was rate-limiting for crystal dissolution.[4] Note that k^+_{Cl} is also several orders of magnitude less than the diffusion-controlled rate constant, that is, 1×10^9 L/mol/s (see Supporting Information). Thus, the quasi-equilibrium assumption for the docking event is appropriate. Table 1 summarizes the computed rate constants.

We can rationalize the rate-limiting role of Cl^- for both growth and dissolution by considering the electrostatic forces that resist the critical formation of a void in the kink site during both ion attachment and detachment. For ion detachment, the ion resists displacement from the kink site, until the void created is large enough for a water molecule to access the kink. The larger Cl^- must move farther out of the kink to admit water than the smaller Na^+; hence, Cl^- detachment limits the dissolution rate. For ion attachment, water must be removed from the kink site to accommodate the incoming ion. Water binds more strongly to the nest of Na^+ ions in a vacant/

DOI: 10.1021/acs.cgd.8b01184
Cryst. Growth Des. 2018, 18, 6302−6306

hydrated Cl^- kink site than to the Cl^- ions in the vacant/hydrated Na^+ kink site (see Figure 3); hence, Cl^- attachment is rate-limiting for growth, because its Na^+ counterions that make the kink nest are strongly hydrated.

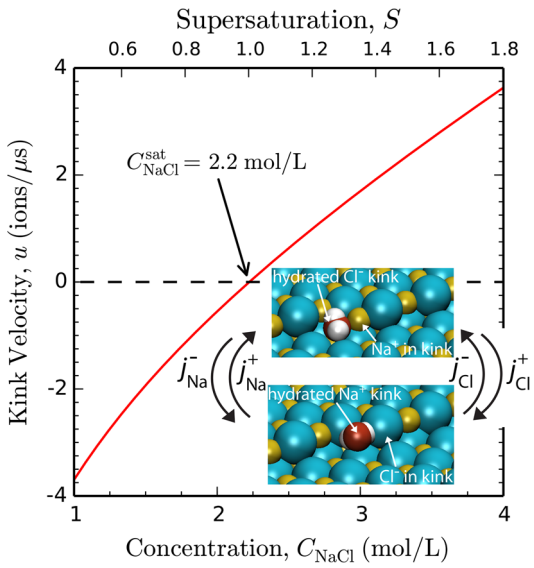

Figure 3. Predicted kink velocity (red) dependence on NaCl concentration. (inset) The kink cycle. For clarity, only the water molecule in the kink is shown to illustrate its coordination with ions in the vacant kink nest.

Our results suggest that ionic crystal growth rates depend on the residence time of water molecules in the solvated kink site, which we anticipate is related to the residence time of water molecules coordinated with ions in solution. In bulk solution, the residence time of water molecules around Na^+ is ~100 times longer than that for Cl^-,[10] which is roughly the difference in our computed attachment rate constants. Our findings provide a specific mechanistic explanation for previous hypotheses that growth rates scale with solvent residence times near ions and surface sites.[11−13] Moreover, our results suggest that accurate correlations for kink attachment rates should consider the maximum residence time of water in all of the relevant environments—the coordination sphere of each bulk solvated ion and at each kink site.

KINK VELOCITY

At nonequilibrium conditions, a kink site progresses through a cycle of alternating Na^+ and Cl^- ions, which is shown in Figure 3. The corresponding kink velocity (number of ions added per time) is

$$u = 2\frac{j^+_{Na}j^+_{Cl} - j^-_{Na}j^-_{Cl}}{j^+_{Na} + j^+_{Cl} + j^-_{Na} + j^-_{Cl}} \quad (4)$$

where the factor of 2 accounts for the two ions in the cycle.[14,15] The computed NaCl kink rate is shown in Figure 3. Over the course of a microsecond, the net motion of a kink is only predicted to be a few ions (at low-to-moderate under/supersaturation), which helps explain why direct coexistence simulations of NaCl and brine require many microseconds to reach equilibrium.[16]

At equilibrium, $u = 0$, which enables a solubility prediction from eq 4 using only our computed rate constants (i.e., without ever computing chemical potentials). We find $C^{sat}_{NaCl} = 2.2 \pm 0.9$ mol/L, which is comparable (Figure 4) to the consensus

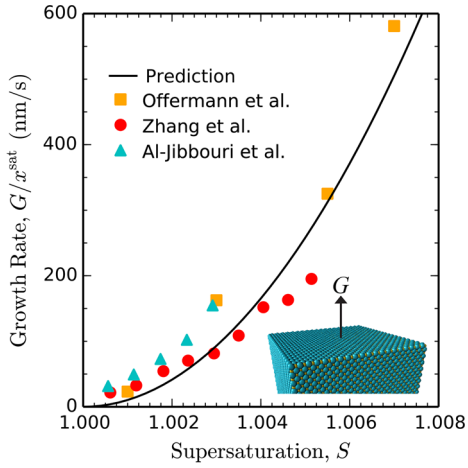

Figure 4. Comparison between our predicted NaCl crystal growth rate and experimental measurements.[32−34]

solubility based on computed chemical potentials for this force field (3.5 ± 0.2 mol/L[17−19] for the NaCl force field of Joung-Cheatham[20] with SPC/E water[21]). Note that the discrepancy between solubility predictions results from a small ($0.5k_BT$) difference in computed free energy differences (i.e., solubility scales exponentially with the free energy difference), where k_B is Boltzmann's constant, and T = 298 K in this work. The experimental solubility is 5.5 mol/L.[22]

KINK DENSITY AND CRITICAL LENGTH

The remaining terms in the growth rate expression are ρ and l_c. These depend on the kink energy ϕ, which characterizes the work required to exchange solvent−solute interactions with solute−solute interactions on the crystal surface (i.e., related to the work required to form a kink site). This exchange of interactions occurs upon ion detachment from a kink site. Thus, from our computed rate constants we calculate the work required for ion detachment ΔW, which yields the kink energy via $\phi = \Delta W/6$ (see Supporting Information). The factor of 6 results from three sets of interactions exchanged (with the three nearest-neighbor ions) and each exchange requiring 2ϕ of work (by convention). The kink energies for Na^+ and Cl^- are $\beta\phi_{Na} = 0.75$ and $\beta\phi_{Cl} = 0.32$, which are in approximate agreement with an experimental estimate, $0.74k_BT$ per ion (note $\beta = 1/k_BT$).[23] A Kossel crystal with these particularly low kink energies would undergo rough growth,[24] but this observation does not directly apply to non-centrosymmetric crystals due to the anisotropic attachment and detachment rates of the different growth units.[25]

These estimates of ϕ suggest that kinks are very prevalent along the edge, consistent with atomic force microscopy studies.[26,27] Traditional kink density models are inappropriate for such a step front, so we employ a model to estimate ρ that treats the complexities of higher kink densities along centrosymmetric edges. We must approximate the NaCl edge as pseudo-centrosymmetric with an average kink energy $\beta\langle\phi\rangle = 0.54$, corresponding to a kinetic kink density of $\rho = 1.2$. A value greater than unity results from multiheight kinks, and we refer interested readers to Joswiak et al. for details.[28]

DOI: 10.1021/acs.cgd.8b01184
Cryst. Growth Des. 2018, 18, 6302−6306

The critical length of a nascent spiral edge corresponds to when it becomes favorable to add an entire new row (i.e., one-dimensional nucleus) to the newly exposed step, $l_c = 2a_E\langle\phi\rangle/\ln S$, where $a_E = 0.28$ nm is the length per ion along the step edge, and the supersaturation is $S = C/C^{sat}$.[29] The critical spiral edge length is 150 nm at $S = 1.002$ and 38 nm at $S = 1.008$. As S increases, l_c continues to decrease. The decrease in l_c with increasing S accelerates growth, but eventually spiral growth gives way to growth by two-dimensional nucleation.[30,31]

NACL CRYSTAL GROWTH RATE

Combining the elementary attachment and detachment rates in the spiral growth model yields in silico NaCl crystal rate growth predictions with no adjustable parameters. We predict G/x^{sat} versus $S = x/x^{sat}$ (x is mole fraction) to remove artifacts from the limited ability of the force field to predict x^{sat}. Note that we are predicting both G and x^{sat}, so an accuracy comparison to the experimental G/x^{sat} values does not mix predicted and observed properties. The in silico predictions yield excellent agreement with measured growth rates.[32−34] Furthermore, our implementation of the spiral growth model is corroborated by the S^2 dependence of the measured growth rates and the ordered step structure found via atomic force microscopy.[27] NaCl growth rates from our calculations and from experiments are of the order of 10 nm/s. This is orders of magnitude faster than the growth rates of other ionic crystals, such as calcite.[11,29] The difference is at least partly reconciled by solubility differences but may also reflect different ion charges and desolvation barriers.

It is important to note that our approach of computing and comparing G/x^{sat} focuses on the predicted kinetics of growth rather than the ability of an atomistic force field to predict the solubility. Computing the saturation concentration of a force field is difficult and time-consuming, and even when the calculation is perfectly done, the result may disagree with the experimental x^{sat} because of force field inaccuracies. However, measuring the solubility in lab is easy. Our strategy enables an accurate "prediction" of G by first predicting the ratio G/x^{sat} and then multiplying G/x^{sat} by the experimentally measured x^{sat}. The resulting predictions for NaCl are shown in Figure S1 of the Supporting Information.

CONCLUSION

In summary, we develop a theoretical framework to compute kink attachment rates, which enables in silico crystal growth rate predictions. For NaCl, we demonstrate that accurate growth rate predictions are possible, even for an imperfect force field. Our results provide a blueprint for connecting atomistic rare event simulations to state-of-the-art crystal growth models and, ultimately, to crystal engineering efforts. The next major milestone will be *rapid* predictions of crystal growth rates via the use of free energy relationships and descriptors including characteristics of the solute, solvent, and kink site(s).

ASSOCIATED CONTENT

Supporting Information

The Supporting Information is available free of charge on the ACS Publications website at DOI: 10.1021/acs.cgd.8b01184.

A comparison of absolute predicted growth rates, details on computing the potentials of mean force, partition functions, diffusion-controlled rate constant, kink detachment work, and on conversion to other concentration measures (PDF)

AUTHOR INFORMATION

Corresponding Authors

*E-mail: baronp@ucsb.edu. Phone: (805) 284-8293. (805) 893-5309. Fax: (805) 893-4731. (B.P.)

*E-mail: mfd@ucsb.edu. (M.F.D.)

ORCID

Mark N. Joswiak: 0000-0002-5237-9484

Michael F. Doherty: 0000-0003-3309-3082

Notes

The authors declare no competing financial interest.

ACKNOWLEDGMENTS

The authors are thankful for financial support from the U.S. National Science Foundation (NSF) (Award Nos. CBET-1335694 and CHE-1465289) and Eli Lilly and Company. The authors acknowledge support from the Center for Scientific Computing from the California NanoSystems Institute and Materials Research Laboratory: an NSF Materials Research Science and Engineering Center (Grant No. DMR-1720256) and NSF Grant No. CNS-1725797.

REFERENCES

(1) Vekilov, P. G. What Determines the Rate of Growth of Crystals from Solution? *Cryst. Growth Des.* **2007**, *7*, 2796−2810.

(2) Stack, A. G.; Raiteri, P.; Gale, J. D. Accurate Rates of the Complex Mechanisms for Growth and Dissolution of Minerals Using a Combination of Rare-Event Theories. *J. Am. Chem. Soc.* **2012**, *134*, 11−14.

(3) Mori, T.; Hamers, R. J.; Pedersen, J. A.; Cui, Q. An Explicit Consideration of Desolvation is Critical to Binding Free Energy Calculations of Charged Molecules at Ionic Surfaces. *J. Chem. Theory Comput.* **2013**, *9*, 5059−5069.

(4) Joswiak, M. N.; Doherty, M. F.; Peters, B. Ion Dissolution Mechanism and Kinetics at Kink Sites on NaCl Surfaces. *Proc. Natl. Acad. Sci. U. S. A.* **2018**, *115*, 656−661.

(5) Dogan, B.; Schneider, J.; Reuter, K. In Silico Dissolution Rates of Pharmaceutical Ingredients. *Chem. Phys. Lett.* **2016**, *662*, 52−55.

(6) Darkins, R. D. W. Computational Insight into the Molecular Mechanisms that Control the Growth of Inorganic Crystals. Ph.D. Thesis, University College London, 2016.

(7) Burton, W. K.; Cabrera, N.; Frank, F. C. The Growth of Crystals and the Equilibrium Structure of their Surfaces. *Philos. Trans. R. Soc., A* **1951**, *243*, 299−358.

(8) Chernov, A. A. The Spiral Growth of Crystals. *Sov. Phys. Usp.* **1961**, *4*, 116−148.

(9) Campbell, C. T. The Degree of Rate Control: A Powerful Tool for Catalysis Research. *ACS Catal.* **2017**, *7*, 2770−2779.

(10) Israelachvili, J. *Intermolecular and Surface Forces;* Academic Press, 2011.

(11) Stack, A. G.; Grantham, M. C. Growth Rate of Calcite Steps As a Function of Aqueous Calcium-to-Carbonate Ratio: Independent Attachment and Detachment of Calcium and Carbonate Ions. *Cryst. Growth Des.* **2010**, *10*, 1409−1413.

(12) Bracco, J. N.; Stack, A. G.; Higgins, S. R. Magnesite Step Growth Rates as a Function of the Aqueous Magnesium:Carbonate Ratio. *Cryst. Growth Des.* **2014**, *14*, 6033−6040.

(13) De La Pierre, M.; Raiteri, P.; Gale, J. D. Structure and Dynamics of Water at Step Edges on the Calcite 10 $\bar{1}$4 Surface. *Cryst. Growth Des.* **2016**, *16*, 5907−5914.

(14) Christiansen, J. A. The elucidation of reaction mechanisms by the method of intermediates in quasi-stationary concentrations. *Adv. Catal.* **1953**, *5*, 311−353.

DOI: 10.1021/acs.cgd.8b01184
Cryst. Growth Des. 2018, 18, 6302−6306

(15) Li, J.; Tilbury, C. J.; Joswiak, M. N.; Peters, B.; Doherty, M. F. Rate Expressions for Kink Attachment and Detachment During Crystal Growth. *Cryst. Growth Des.* **2016**, *16*, 3313−3322.
(16) Espinosa, J. R.; Young, J. M.; Jiang, H.; Gupta, D.; Vega, C.; Sanz, E.; Debenedetti, P. G.; Panagiotopoulos, A. Z. On the Calculation of Solubilities via Direct Coexistence Simulations: Investigation of NaCl Aqueous Solutions and Lennard-Jones Binary Mixtures. *J. Chem. Phys.* **2016**, *145*, 154111.
(17) Benavides, A. L.; Aragones, J. L.; Vega, C. Consensus on the Solubility of NaCl in Water from Computer Simulations Using the Chemical Potential Route. *J. Chem. Phys.* **2016**, *144*, 124504.
(18) Nezbeda, I.; Moučka, F.; Smith, W. R. Recent Progress in Molecular Simulation of Aqueous Electrolytes: Force Fields, Chemical Potentials and Solubility. *Mol. Phys.* **2016**, *114*, 1665−1690.
(19) Mester, Z.; Panagiotopoulos, A. Z. Temperature-Dependent Solubilities and Mean Ionic Activity Coefficients of Alkali Halide in Water from Molecular Dynamics Simulations. *J. Chem. Phys.* **2015**, *143*, 044505.
(20) Joung, I. S.; Cheatham, T. E., III Determination of Alkali and Halide Monovalent Ion Parameters for Use in Explicitly Solvated Biomolecular Simulations. *J. Phys. Chem. B* **2008**, *112*, 9020−9041.
(21) Berendsen, H. J. C.; Grigera, J. R.; Straatsma, T. P. The Missing Term in Effective Pair Potentials. *J. Phys. Chem.* **1987**, *91*, 6269−6271.
(22) Hamer, W. J.; Wu, Y. C. Osmotic Coefficients and Mean Activity Coefficients of Uni-univalent Electrolytes in Water at 25°C. *J. Phys. Chem. Ref. Data* **1972**, *1*, 1047−1099.
(23) Christoffersen, J.; Rostrup, E.; Christoffersen, M. R. Relation Between Interfacial Tension of Electrolyte Crystals in Aqueous Suspension and their Solubility; a Simple Derivation Based on Surface Nucleation. *J. Cryst. Growth* **1991**, *113*, 599−605.
(24) Onsager, L. Crystal Statistics. I. A Two-Dimensional Model with an Order-Disorder Transition. *Phys. Rev.* **1944**, *65*, 117−149.
(25) Cuppen, H. M.; Meekes, H.; van Enckevort, W. J. P.; Vissers, G. W. M.; Vlieg, E. Kinetic Roughening of Kossel and Non-Kossel Steps. *Surf. Sci.* **2004**, *569*, 33−46.
(26) Shindo, H.; Ohashi, M.; Tateishi, O.; Seo, A. Atomic Force Microscopic Observation of Step Movements on NaCl(001) and NaF(001) with the Help of Adsorbed Water. *J. Chem. Soc., Faraday Trans.* **1997**, *93*, 1169−1174.
(27) Bode, A. A. C.; Jiang, S.; Meijer, J. A. M.; van Enckevort, W. J. P.; Vlieg, E. Growth Inhibition of Sodium Chloride Crystals by Anticaking Agents: In Situ Observation of Step Pinning. *Cryst. Growth Des.* **2012**, *12*, 5889−5896.
(28) Joswiak, M. N.; Peters, B.; Doherty, M. F. Nonequilibrium Kink Density from One-Dimensional Nucleation for Step Velocity Predictions. *Cryst. Growth Des.* **2018**, *18*, 723−727.
(29) Teng, H. H.; Dove, P. M.; Orme, C. A.; De Yoreo, J. J. Thermodynamics of Calcite Growth: Baseline for Understanding Biomineral Formation. *Science* **1998**, *282*, 724−727.
(30) Tilbury, C. J.; Doherty, M. F. Modeling Layered Crystal Growth at Increasing Supersaturation by Connecting Growth Regimes. *AIChE J.* **2017**, *63*, 1338.
(31) Lovette, M. A.; Doherty, M. F. Predictive Modeling of Supersaturation-Dependent Crystal Shapes. *Cryst. Growth Des.* **2012**, *12*, 656−669.
(32) Offermann, H.; von Brachel, G.; Al-Sabbagh, A.; Farelo, F. Crystallization Kinetics of NaCl in Multicomponent Solutions. *Cryst. Res. Technol.* **1995**, *30*, 651−658.
(33) Zhang, S. B.; Yuan, J. J.; Mohameed, H. A.; Ulrich, J. The Effect of Different Inorganic Salts on the Growth Rate of NaCl Crystallized from Sea Water. *Cryst. Res. Technol.* **1996**, *31*, 19−25.
(34) Al-Jibbouri, S.; Ulrich, J. The Growth and Dissolution of Sodium Chloride in a Fluidized Bed Crystallizer. *J. Cryst. Growth* **2002**, *234*, 237−246.

DOI: 10.1021/acs.cgd.8b01184
Cryst. Growth Des. 2018, 18, 6302−6306